APPENDIX VII

Publication P7

Burakov, A., Arkkio, A. 2007. Comparison of the unbalanced magnetic pull mitigation by the parallel paths in the stator and rotor windings. *IEEE Transactions on Magnetics*, in press.

Comparison of the Unbalanced Magnetic Pull Mitigation by the Parallel Paths in the Stator and Rotor Windings

Andrej Burakov and Antero Arkkio

Abstract—**The eccentric rotor causes an electromagnetic force acting between the rotor and stator of an electrical machine. This force tries to further increase the rotor eccentricity and may severely degrade the performance of the machine causing acoustic noise, vibration, excessive wear of bearing, rotor and stator rubbing and etc. Parallel connections are long known as being a simple and yet effective remedy for the problems associated with rotor eccentricity. In this work, two common types of electrical machine running with eccentric rotor are investigated. Operation in a wide whirling frequency range is considered. The effects of parallel connections in the stator and rotor windings on the eccentricity force are studied numerically and compared to each other. Results of this project reveal that the parallel stator windings can be more effective in mitigating the unbalanced magnetic pull than the rotor cage (or damper winding), which, normally, has many more parallel circuits.**

Index Terms—**Induction machines, synchronous generators, vibrations, finite element methods, unbalanced magnetic pull.**

I. Introduction

An ECCENTRIC rotor motion (also called 'rotor whirling') occurs when the rotor axis of an electrical machine does not coincide with the axis of the stator bore but, instead, travels around the latter at a certain radius and angular speed (called 'whirling radius' and 'whirling angular speed', respectively). Due to manufacturing tolerances, wear of bearings and other reasons, some degree of rotor eccentricity is always present. Rotor whirling generates the electromagnetic force (also known as unbalanced magnetic pull, UMP) that acts between the rotor and stator. This force can be resolved into two components: the radial one, acting in the direction of the shortest air gap; and the tangential one, which is perpendicular to the radial one. The amplitude and direction of this force depend on the operating characteristics of the motor, whirling frequency and radius. Acting roughly in the direction of the shortest air gap, the UMP tries to further increase the eccentricity magnitude and may cause a serious damage to the machine or even the whole drive. Besides, UMP acts also as a source of vibration and acoustic noise.

The occurrence and effects of an eccentric rotor in electrical machine have been discussed for more than one hundred years [1], and the beneficial effects of parallel windings in mitigating the resultant UMP have been discussed almost as long [2].

Most commonly, two particular cases of the eccentric rotor motion were investigated: namely, the static and dynamic eccentricity. Static eccentricity implies that the eccentric-rotor axis does not move with respect to the stator, i.e. the whirling frequency is zero. Whereas, in case of dynamic eccentricity, rotor axis whirls around the stator bore axis at a frequency of the mechanical rotor motion. However, according to [3], the whirling motion of the rotor can also have other frequencies.

Analytical methods have commonly been used to study the electromagnetic forces due to the rotor eccentricity. In [4], an early attempt was made to analytically describe the UMP due to the static rotor eccentricity in induction and synchronous machines. Using the analytical approach, in [5], it was shown that the parallel connections in the stator winding can effectively reduce the UMP magnitude and also cause the shift of the UMP direction from that of the eccentricity. In an analytical model for induction machine with dynamic eccentricity, developed in [6], the UMP mitigation by the currents circulating in the parallel paths of the stator winding was accounted for by introducing the corresponding damping coefficient.

Though being extensively used, the analytical methods had difficulties when accurate evaluation of the equalizing currents, the effects of saturation and stator and rotor slotting was needed. These problems were solved by applying numerical techniques. In [7], the radial forces on an eccentric rotor of a cage induction motor were calculated using time-stepping finite element analysis (FEA). The iron core saturation and currents circulating in the rotor cage and parallel paths of the stator winding were all accounted for in the calculation. The UMP mitigation by the currents circulating in various arrangements of the parallel stator windings was also numerically studied in [8]. In [9], the magnetic field harmonics engendered by the rotor eccentricity were evaluated in a wide whirling frequency range by applying the numerical impulse response test in the FEA. Using numerical analysis in [10], the authors were able to resolve the total electromagnetic force due to the eccentric rotor into several constituents: those related to the fundamental field, stator and rotor slotting and higher harmonics.

Combining the precision of FEA with the lucidity of analytical approach was attempted in [11], where a simple parametric model was introduced to accurately represent the

Manuscript received on March 14, 2007.
A. Burakov (phone: +358 9 451 2381, e-mail: Andrej.Burakov@tkk.fi).
A. Arkkio (e-mail: Antero.Arkkio@tkk.fi).
Authors are with Helsinki University of Technology, Laboratory of Electromechanics, P.O. Box 3000, FIN-02015 HUT, Espoo, Finland.

UMP on the eccentric rotor of electrical machine with parallel stator windings. This model with parameters estimated from the results of numerical simulation, performed very well in a wide whirling frequency range, when applied to induction machine and a salient-pole synchronous machine.

In this work, the effects of the rotor cage (or damper winding) and parallel stator windings on the UMP due to the eccentric rotor are investigated numerically and compared to each other. Unlike most of the papers published on the topic, this study is not only concerned with induction machine, but examines also another common machine type – the synchronous machine. Besides, the analysis presented in this paper is not limited to special cases of static and/or dynamic eccentricity but covers a wide whirling frequency range. Operation in wide whirling frequency range becomes particularly important when studying the electromechanical interactions in electrical machine.

The findings of this study show that in the whirling frequency range investigated, the behaviour of the UMP is determined mostly by the magnetic field harmonics introduced by the rotor eccentricity. The acquired results demonstrate that two parallel stator windings unevenly reduce the UMP on the orthogonal axes. The rotor cage is shown to effectively attenuate the UMP without causing its asymmetry. Interestingly, in both test machines, four parallel stator windings prove to be more effective in mitigating the UMP than the rotor cage. As expected, the electrical machines incorporating parallel circuits both in the rotor and in the stator operate with the smallest amount of UMP.

II. Methods of Analysis

A. Basic theory explaining the UMP mitigation by the parallel circuits

In electrical machine with p pole-pairs, the fundamental component of the magnetomotive force (MMF) can be represented as

$$F_p^{\mathrm{s}}(\varphi,\ t) = \mathrm{Re}\left\{F_{p,\max}\mathrm{e}^{\mathrm{j}(p\varphi-\omega_1 t)}\right\}, \qquad (1)$$

here, $F_{p,\max}$ is amplitude of the fundamental MMF component; j is imaginary unit; φ is angular coordinate; ω_1 is angular frequency of the supply voltage; t denotes time; superscript "s" indicates that a stator reference frame is used; Re indicates the real part of the corresponding quantity.

For cylindrical rotor machine with cylindrical circular rotor eccentricity the air gap is described as follows

$$\delta^{\mathrm{s}}(\varphi,\ t) = \mathrm{Re}\left\{\delta_{\mathrm{e}} + \delta_{\mathrm{ecc}}\mathrm{e}^{\mathrm{j}(\varphi-\omega_{\mathrm{ecc}}t+\varphi_{\mathrm{ecc.0}})}\right\}, \qquad (2)$$

here, δ_{e} is nominal air gap, which also accounts for the effect of tooth saturation; δ_{ecc} is whirling radius; ω_{ecc} is whirling angular speed; $\varphi_{\mathrm{ecc.0}}$ is initial phase angle of the rotor eccentricity.

The air gap permeance is calculated as

$$\lambda^{\mathrm{s}}(\varphi,\ t) = \mu_0 / \delta^{\mathrm{s}}(\varphi,\ t), \qquad (3)$$

here, μ_0 is permeability of free space.

Substituting (2) into (3) results in a Fourier series where the most prominent components have wave-numbers 0 (constant term) and 1

$$\lambda^{\mathrm{s}}(\varphi,\ t) = \frac{\mu_0}{\delta_{\mathrm{e}}}\left(1 - \frac{1}{\delta_{\mathrm{e}}}\mathrm{Re}\left\{\delta_{\mathrm{ecc}}\mathrm{e}^{\mathrm{j}(\varphi-\omega_{\mathrm{ecc}}t+\varphi_{\mathrm{ecc.0}})}\right\}\right). \qquad (4)$$

From (1) and (4) the magnetic flux density is obtained

$$B^{\mathrm{s}}(\varphi,\ t) = F^{\mathrm{s}}(\varphi,\ t)\cdot\lambda^{\mathrm{s}}(\varphi,\ t). \qquad (5)$$

Thus,

$$B^{\mathrm{s}}(\varphi,\ t) = F_{p,\max}\frac{\mu_0}{\delta_{\mathrm{e}}}\mathrm{Re}\left\{\mathrm{e}^{\mathrm{j}(p\varphi-\omega_1 t)} - \frac{\delta_{\mathrm{ecc}}}{2\delta_{\mathrm{e}}}\left(\mathrm{e}^{\mathrm{j}((p-1)\varphi-(\omega_1-\omega_{\mathrm{ecc}})t-\varphi_{\mathrm{ecc.0}})} + \mathrm{e}^{\mathrm{j}((p+1)\varphi-(\omega_1+\omega_{\mathrm{ecc}})t+\varphi_{\mathrm{ecc.0}})}\right)\right\}. \qquad (6)$$

As seen from (6), rotor eccentricity distorts the magnetic flux density distribution in the air gap by introducing additional magnetic flux density harmonics. These harmonics (also called 'eccentricity harmonics') have wave-numbers $p\pm1$ and rotate at angular speeds $\omega_1 \pm \omega_{\mathrm{ecc}}$, respectively. When interacting with the fundamental magnetic field component, these eccentricity harmonics produce the UMP.

In general case, eccentricity harmonics induce voltages and, hence, circulating currents in the parallel paths of the rotor and stator windings. The circulating currents reduce the original eccentricity harmonics and mitigate the resultant UMP. However, at certain whirling frequencies, the eccentricity fields become stationary with respect to the rotor or stator. In these cases, they induce neither voltages nor currents in the parallel windings and their magnitudes and also the UMP rise. It can be deduced from (6) that $p\pm1$ eccentricity harmonics are stationary with respect to the rotor at whirling angular speeds $\omega_{\mathrm{ecc}} = \omega_1(\mp s + (1-s)/p)$, respectively. In this equation, symbol s denotes the slip of the rotor. As the frequency notation is used hereafter, this last expression can be rewritten as, $f_{\mathrm{ecc}} = f_1(\mp s + (1-s)/p)$, where f_1 is supply frequency and f_{ecc} is whirling frequency. When the whirling frequency is $f_{\mathrm{ecc}} = \mp f_1$, $p\pm1$ magnetic flux density harmonics are stationary with respect to the stator winding.

Thus, when electrical machine is equipped with parallel paths in the rotor, the $p\pm1$ eccentricity harmonics and UMP are expected to peak at whirling frequencies $f_{\mathrm{ecc}} = f_1(\mp s + (1-s)/p)$. If there are parallel paths in the stator, the eccentricity harmonics and UMP will peak at $f_{\mathrm{ecc}} = \mp f_1$. In case the parallel paths are present both, in the rotor and stator windings, the peaks are to be observed at all the whirling frequencies of the two separate cases mentioned above. These statements are confirmed by the numerical simulation results shown in Fig. 1.

Fig. 1 illustrates the Frequency Response Functions (FRFs) of the eccentricity harmonics that occur in eight-pole

50 Hz synchronous machine with eccentric rotor. Table I lists more data on this machine. As the performance of electrical machine was studied in a wide whirling frequency range ([–100, 100] Hz), the results of numerical simulations are presented, using the FRF notation. The FRF represents the quantity of interest (in this case, magnetic flux density harmonics) per whirling radius as a function of whirling frequency (see Fig. 1), thus, allowing for a very compact representation of the data.

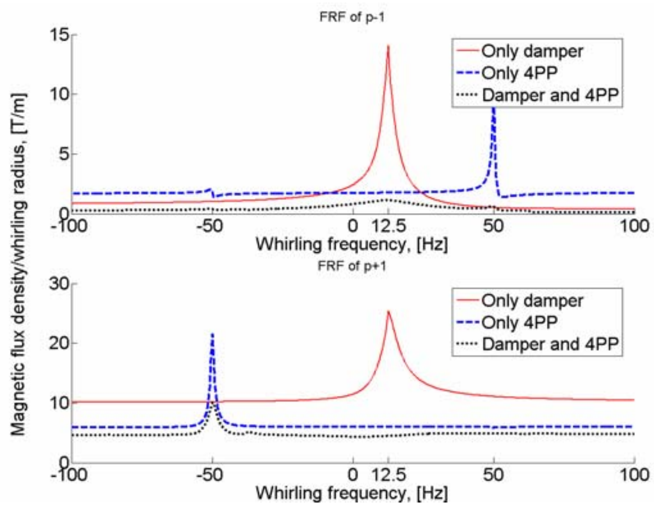

Fig. 1. FRFs of the eccentricity harmonics in eccentric-rotor synchronous machine.

In the legends of Fig. 1, "4PP" stands for Four Parallel Paths in the stator winding.

The upper plot in Fig. 1 shows the FRFs of the magnetic flux density harmonic with wave-number p–1, whereas, the lower plot illustrates the FRFs of the magnetic flux density harmonic with wave-number p+1. Absolute values of the eccentricity harmonics were utilized to calculate these FRFs. In both plots it is seen that in a machine, which only has a damper winding (continuous curves), both eccentricity harmonics peak at the whirling frequency $f_{ecc} = f_1\left(\mp s + (1-s)/p\right)$, which in this example is 12.5 Hz (f_1 = 50 Hz, s = 0, p = 4). If the machine is equipped with parallel stator windings only (dashed curves), the $p\pm1$ magnetic field harmonics peak at whirling frequency $f_{ecc} = \mp f_1 = \mp 50$ Hz, respectively. And finally, in the machine with parallel paths both in the rotor and stator (dotted curves), the eccentricity harmonics peak at the whirling frequency values of 12.5 Hz and $\mp$ 50 Hz.

Results presented in Fig. 1 agree very well with the theoretical analysis presented earlier in this paper.

As will be shown later, these peaks in the eccentricity harmonics can also be seen in the FRFs of the electromagnetic force.

B. Numerical calculation of the magnetic field

The computation of the magnetic field employed in this work was based on the transient time-stepping FEA [12]. The magnetic field and circuit equations were discretized and solved together as a system of equations. The time-dependence of the variables was modeled by Crank-Nicholson method. The forces were calculated at each time-step using a method developed by Coulomb [13].

Several simplifications were made in order to reduce the amount of computation. The magnetic field in the core region was assumed to be two-dimensional. The laminated iron core was treated as a non-conducting magnetically non-linear medium, and the non-linearity was modeled by a single-valued magnetization curve. Modeling of the air gap regions also was two-dimensional. The rotor motion was facilitated by changing the shapes of the finite elements (FE) in the air gap.

All numerical calculations were carried out on a PC powered by AMD Athlon 64 3000+ processor. Synchronous machine was simulated using first order FE. The FE model contained 7344 nodes. Two seconds of the machine performance required three hours of computation time. Induction machine was simulated using second order FE; its model contained 8677 nodes. To simulate one second of the machine operation required approximately five hours of computation time.

The numerical analysis used in this work was verified by measurements in [14].

III. Results

Two common types of electrical machine were studied: 1) a cage induction machine; 2) a salient-pole synchronous machine. Table I lists the most important data of these machines.

The performance of the induction machine with three different stator winding arrangements was investigated:

1. series connection (no parallel paths);
2. two parallel paths;
3. four parallel paths.

TABLE I
MAIN PARAMETERS OF THE MACHINES INVESTIGATED

Parameter \ Machine type	Induction machine	Synchronous machine
Number of pole-pairs	2	4
Rated frequency, [Hz]	50	50
Rated stator voltage, [V]	380	6300
Rated power, [kW]	15	8200
Rated slip	0.032	–
Number of rotor slots	34	32
Connection	Delta	Star
Skew of the rotor slots	0	0

In order to assess the influence of the rotor cage on the UMP magnitude, the stator winding was connected in series. The effects of the parallel stator windings were studied when there were no bars in the rotor cage (rotor cage material switched to "air" in the FEA). The stator winding with two parallel paths was assembled in such a way that two neighbouring poles were connected in series and the opposite poles in parallel. According to [8], motors with stator windings assembled in such a way would run more quietly than those with neighboring poles in parallel and opposite poles in series.

In Fig. 2, the FRFs of the eccentricity force in the induction machine operated at no load are presented. As the UMP consists of two components, the FRFs were also resolved into two constituents: the radial one and the tangential one. This representation allows to conveniently assess the magnitude and direction of the electromagnetic forces at every whirling frequency value, within the whole whirling frequency range of interest.

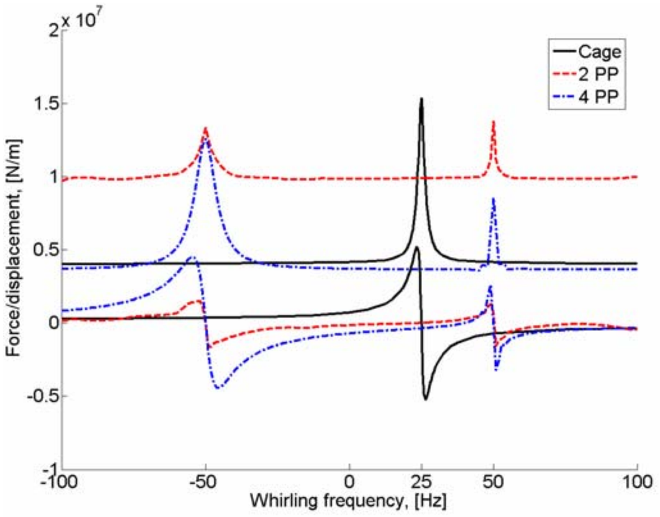

Fig. 2. Comparison of the FRFs of the force in the induction machine.

The three upper curves in Fig. 2 represent the radial components of the electromagnetic force, whereas, the three lower curves correspond to the tangential electromagnetic force components. The radial and tangential force components rotate together with the point of the shortest air gap at the whirling frequency indicated on X-axis.

Fig. 3 shows the absolute values of the three FRFs of the force plotted in Fig. 2.

In Fig. 4, the traces of the electromagnetic force acting on an eccentric rotor of the induction machine at a whirling frequency of –25 Hz are shown. The whirling radius during these simulations was 20% of the average air gap length.

The FRFs of the force when the induction machine was equipped with both the rotor cage and parallel paths in the stator winding are presented in Fig. 5. These are also compared with the FRF when machine had only four parallel stator windings.

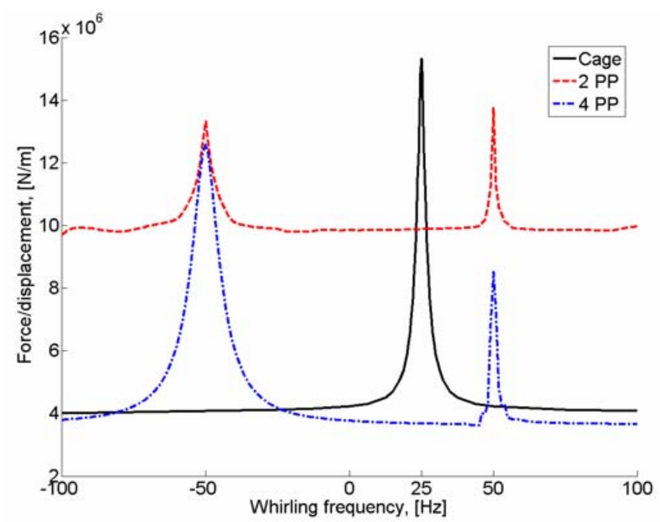

Fig. 3. Absolute values of the FRFs of the force in the induction machine.

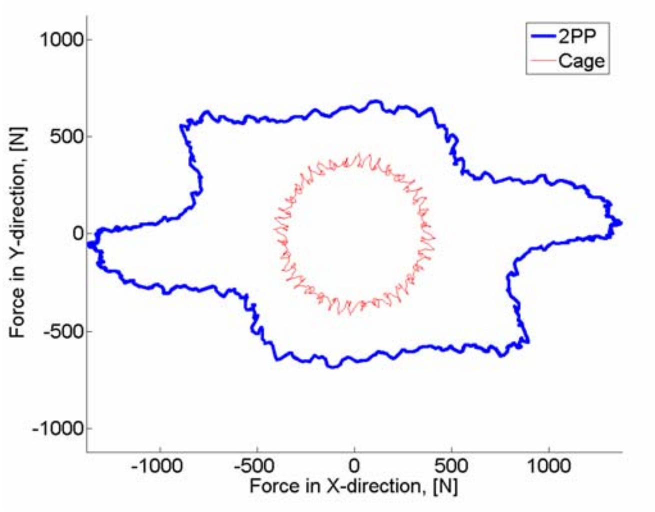

Fig. 4. Electromagnetic force trace: induction machine at no load, whirling frequency –25 Hz, whirling radius 20% of the air gap.

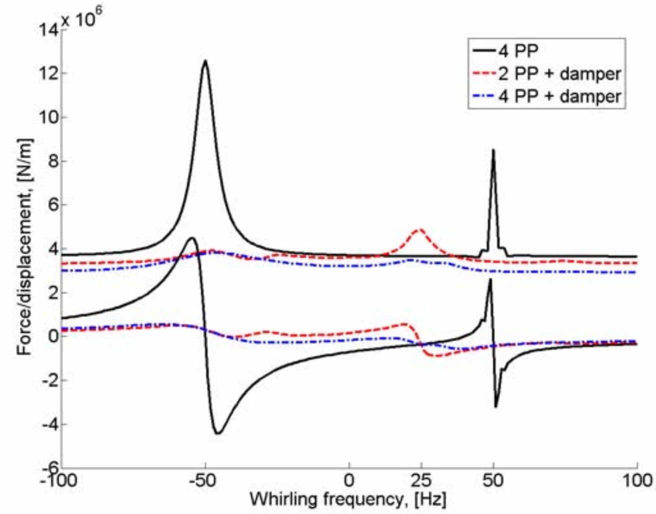

Fig. 5. The FRF of the force when induction machine has both the rotor cage and parallel stator windings.

In Fig. 6, the FRFs of the force acting on the eccentric rotor of synchronous machine are shown. The machine was simulated at rated load. Three cases were studied:

1. machine with stator winding connected in series and with the damper winding;
2. four parallel stator windings;
3. four parallel stator windings and the damper winding.

IV. Discussion

In [15], it is mentioned that the frequency of the eccentricity force is often smaller than that of the fundamental field. As this work is focused on the electromagnetic forces created by rotor eccentricity, the whirling frequency range of interest was chosen to be [–100, 100] Hz. A negative whirling frequency implies that the point of the shortest air gap travels in the direction opposite to that of the mechanical rotor motion.

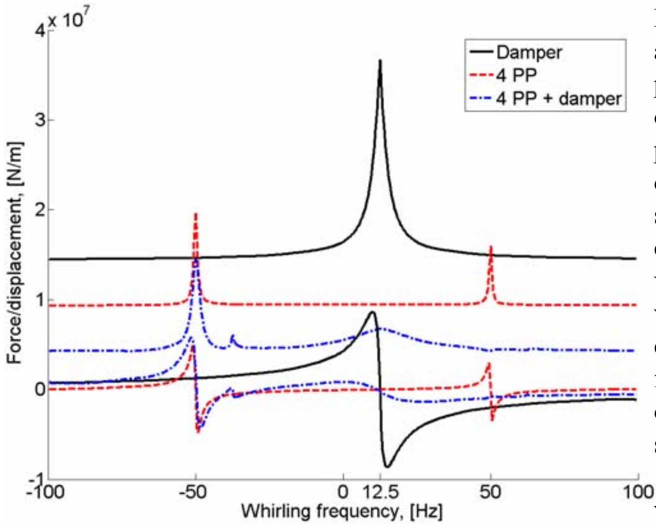

Fig. 6. Comparison of the FRFs of the force in synchronous machine.

Although the application of an induction machine having parallel stator windings and operating without the rotor cage may, in real life, not be practical, it still is possible. Nonetheless, simulation results of such a machine provided important information on the UMP mitigation by the parallel stator windings.

Results presented in Fig. 1 demonstrate that $p+1$ eccentricity harmonic is substantially stronger than the $p-1$ harmonic. It is also seen that four parallel stator windings reduce the former harmonic to a significantly lower level than the damper winding alone. By using the parallel paths in the rotor and stator windings simultaneously, both eccentricity harmonics are reduced the most.

According to the results presented in Figs. 2 and 3, the strongest UMP will occur when the induction machine has two parallel stator windings. The rotor cage alone provides a considerably more effective magnetic force reduction than the two parallel stator windings. It is important to note that in the whirling frequency range studied, four parallel stator windings ensure the smallest average value of the radial UMP component, the tangential component, though, being stronger than in the other two configurations. This observation agrees with statement in [5], declaring that parallel stator windings cause the UMP direction to shift from the eccentricity axis. Comparing the absolute UMP values, shown in Fig. 3, it is seen that in the whirling frequency range [–100, 100] Hz, the smallest average value of the UMP corresponds to the induction machine with four parallel stator windings. Note also that the radial FRF components peak at the whirling frequency of ±50 Hz (supply frequency), when there are parallel stator windings. In case of rotor cage, the radial FRF component peaks at a whirling frequency 25 Hz (mechanical angular frequency of the rotor). This UMP behavior is attributed to the magnetic field harmonics initiated by the rotor eccentricity. At ±50 Hz, these eccentricity harmonics are stationary with respect to the stator winding and are not affected by the latter. Similar phenomenon occurs at 25 Hz, when the eccentricity harmonics are not being damped by the rotor cage.

When investigating the induction machine equipped with two parallel stator windings, the FEA results revealed that the eccentricity force vector has an elliptic trajectory (see Fig. 4), even though the rotor axis traveled at a circular orbit around the stator bore axis. It was concluded that two parallel stator windings cause uneven UMP damping on the orthogonal axes. This finding conforms well to the results presented in [4], wherein, it is stated that there is no damping of the UMP along the line between the two parallel stator windings. The FRF curves for this machine configuration were calculated taking the average force values over a certain time interval. When induction machine was equipped with the damper winding only, the eccentricity force vector had almost circular trace, except for the small ripples due to slotting (see Fig. 4). The operation with four parallel stator windings provided a very similar UMP trace and, thus, is not presented here.

The induction machine incorporating parallel stator windings and rotor cage was expected to have even stronger UMP mitigation than when it had only either of these. Indeed, as shown in Fig. 5, using two parallel stator windings along with the rotor cage provided a considerably smaller UMP magnitude than the one corresponding to the machine with four parallel stator windings alone. Both, the radial and tangential UMP components were reduced substantially. Adding two more parallel paths to the stator winding provided a further reduction of the UMP magnitude in the whole whirling frequency range studied.

When investigating the synchronous machine (Fig. 6), the strongest UMP was obtained for the machine equipped with the damper winding only. Employing four parallel stator windings instead of the damper winding allowed for a significant reduction of the radial and tangential UMP components. When the parallel stator windings and damper winding were applied together, the smallest FRF of the force was recorded. It is important to mention that when the machine has parallel paths both in the rotor and stator, the FRF of the force contains the traces of the two corresponding FRFs (note the peaks in the radial FRF at ±50 and 12.5 Hz). Besides, there also are new phenomena due to the coupling of the currents circulating in the rotor with those circulating in the stator, which result in additional peaks in the radial FRF curve (at –37.5 and 62.5 Hz).

Results presented in Figs. 1 and 6 also show that peaks in the magnetic flux density harmonics and in the UMP have very similar shape and occur at the same frequency. From this observation a conclusion can be made that in the whirling frequency range studied, the FRF of the force has the behaviour, which is determined mostly by the eccentricity harmonics.

Another important observation seen in Figs. 5 and 6 is that when the machine is equipped with parallel paths in the stator and rotor, not only the average level of the UMP is lessened but also the magnitudes of the peaks in the FRF, coming from each individual winding, are reduced significantly.

The results of this work could not corroborate the statement in [15] claiming that parallel stator windings are less effective than the rotor cage in reducing the UMP as the rotor cage contains many more parallel circuits. According to our calculation results, presented in Figs. 2, 3 and 6, four parallel stator windings are capable of providing stronger UMP mitigation than the rotor cage (damper winding), where there were 34 parallel circuits in induction machine and 32 in synchronous machine.

V. Conclusions

In this work, two common types of electrical machines operating with eccentric rotor were studied. The effects of parallel connections in the rotor cage (damper winding) and stator winding on the UMP were investigated numerically in a wide whirling frequency range. It was shown that in the whirling frequency range [–100, 100] Hz, the behaviour of the UMP is determined mostly by the eccentricity harmonics. The acquired results demonstrated that two parallel stator windings unevenly reduce the UMP on the orthogonal axes. The rotor cage was shown to effectively attenuate the UMP without causing its asymmetry. Interestingly, in both test machines, four parallel stator windings proved to be more effective in mitigating the UMP than the rotor cage. As expected, the electrical machines incorporating parallel circuits both in the rotor and in the stator operated with the smallest amount of UMP.

VI. References

[1] J. Fisher-Hinnen, “Dynamo design”, Van Nostrand, 1899.

[2] R. E. Hellmund, “Series versus parallel windings for a.c. motors”, Electrical World, No. 49, 1907, pp. 388 – 389.

[3] A. Tenhunen, T. P. Holopainen, A. Arkkio, “Impulse method to calculate the frequency response of the electromagnetic forces on whirling cage rotors”, *IEE Proceedings, Electrical Power Applications*, Vol. 150, No. 6, November 2003, pp. 752 – 756.

[4] R. C. Robinson, “The calculation of unbalanced magnetic pull in synchronous and induction motors”, *AIEE Transactions*, Vol. 62, October 1943, pp. 620 – 624.

[5] D. G. Dorrell, A. C. Smith, “Calculation of UMP in induction motors with series or parallel winding connections”, *IEEE Transactions on Energy Conversion*, Vol. 9, No. 2, June 1994, pp. 304 – 310.

[6] A. Stavrou, J. Penman, “Modelling dynamic eccentricity in smooth air-gap induction machines”, Electric Machines and Drives Conference, 2000, IEMDC 2001, IEEE International, 2001, pp. 864 – 871.

[7] A. Arkkio, “Unbalanced magnetic pull in cage induction motors – dynamic and static eccentricity”, Proceedings of the International Conference on Electrical Machines, 10-12 September 1996, Vigo, Spain, pp. 192 – 197.

[8] M. J. DeBortoli, S. J. Salon, D. W. Burow and C. J. Slavik, “Effects of rotor eccentricity and parallel windings on induction machine behaviour: a study using finite element analysis”, *IEEE Transactions on Magnetics*, Vol. 29, No. 2, March 1993, pp. 1676 – 1682.

[9] A. Tenhunen, “Calculation of eccentricity harmonics of the air-gap flux density in induction machines by impulse method”, *IEEE Transactions on Magnetics*, May 2005, Vol. 41, No. 5, pp. 1904-1907.

[10] P. Frauman, A. Burakov, A. Arkkio, “Effects of the slot harmonics on the unbalanced magnetic pull in an induction motor with an eccentric rotor”, *IEEE Transactions on Magnetics*, August 2007, Vol. 43, No. 8, pp. 3441-3444.

[11] A. Burakov, A. Arkkio, “Low-order parametric force model for eccentric-rotor electrical machine with parallel connections in stator winding”, *IEE Proceedings, Electric Power Applications*, Vol. 153, Issue 4, July 2006, pp. 592-600.

[12] A. Arkkio, “Analysis of induction motors based on the numerical solution of the magnetic field and circuit equations”, *Acta Plytechnica Scandinavica, Electrical Engineering Series*, 1987, No. 59, Helsinki 97p.

[13] J. L. Coulomb, “A methodology for the determination of global electromechanical quantities from a finite element analysis and its application to the evaluation of magnetic forces, torques and stiffness”, *IEEE Transactions on Magnetics*, Vol. 19, No. 6, Nov. 1983, pp 2514 – 2519.

[14] A. Arkkio, M. Antila, K. Pokki, A. Simon and E. Lantto, “Electromagnetic force on a whirling cage rotor”, *IEE Proceedings, Electric Power Applications*, vol.147, Sept. 2000, pp. 353 – 360.

[15] D. G. Dorrell, “Calculation of unbalanced magnetic pull in small cage induction motors with skewed rotors and dynamic rotor eccentricity”, *IEEE Transactions on Energy Conversion*, Vol. 11, No. 3, September 1996, pp. 483 – 488.

VII. Biographies

Andrej Burakov was born in Panevėžys, Lithuania on March 3, 1979. In 2001, he acquired the B.Sc. (Tech.) degree from Vilnius Gediminas technical university. In 2003, he received the M.Sc. (Tech.) degree from Helsinki University of Technology.

He is currently working in Helsinki University of Technology as a research scientist pursuing the D.Sc. (Tech.) degree. His research interests involve modeling and numerical analysis of electrical machines operating with eccentric rotors.

Antero Arkkio was born in Vehkalahti, Finland, in 1955. He received the MSc (Tech) and DSc (Tech) degrees from Helsinki University of Technology (TKK) in 1980 and 1988, respectively.

He has worked with various research projects dealing with modeling, design and measurement of electrical machines. He has been Professor of Electrical Engineering (Electromechanics) at TKK since 2001.